WAVE BASED APPROACH TO COASTAL BATHYMETRY- CASE STUDIES OF COASTAL REGIONS IN INDIA

Ankita Misra (1), Balaji Ramakrishnan (1), Amit More (2)

[1] Indian Institute of Technology- Bombay
[2]Honda R&D Co Ltd.
Email: ankitamisra1987@gmail.com

KEY WORDS: Wave based Approach (WBA), Synthetic aperture radar, Fast Fourier Transform, Linear Dispersion Equation, bathymetry

ABSTRACT: Synthetic Aperture radar is an all-weather and time active sensor that emits radiation in the microwave region of the spectrum. The backscattered patterns depicted by the SAR image of the sea surface are the measure of the sea surface roughness and when combined with the study of swell wave transformation can be used to estimate the bottom topography. In this study, swell wave shoaling and refraction phenomenon are used on ALOS PALSAR Dual Pol HH polarized SAR data of 12.5m resolution of 16th June 2007 and 26th January 2007 to derive bathymetry for the coastal regions in Maharashtra and Puducherry respectively. The wave based approach (WBA) applied here is a simplified algorithm that assumes that the swell waves are perfectly imaged by SAR without any disturbances and can retrieve depths in the range of 10 – 40 m using the linear dispersion equation. After initial pre-processing of SAR imagery, the methodology includes spectral analysis and application of linear dispersion equation, which are conducted using a raster approach, which involves moving a scanning window along the image axes. Based on the results obtained, it is seen that the swell wavelength in both the study regions show a general decreasing trend while moving toward the shoreline. For Maharashtra region, the swell wavelength is found to be in the range of 130–250 m and the water depth at the farthest point (almost 47 km away from shoreline) is estimated to be 45m. On further validation of the data with 450 points obtained from admiralty charts a R^2 value of 0.98 is obtained with a Root Mean Square Error (RMSE) of 1.1m and Mean Absolute Error (MAE) of 0.97m. Also on comparison with GEBCO data, the same points give a R^2 of 0.97 with a RMSE of 1.34m and MAE of 1.1m. Furthermore, in case of Puducherry, the swell wavelength is found to be in the range of 120–350 m. The water depth at the farthest point (almost 11 km away from shoreline) is observed to be 30m, and on validation with 195 GEBCO points an R^2 value of 0.97 is obtained with a RMSE of 0.83 m and MAE of 0.66m. It can therefore be inferred that this SAR based approach can be utilized to derive depths for coastal regions as well as can be combined with optical remote sensing data to derive bathymetry maps with greater spatial coverage and resolution. This will thereby contribute to long-term coastal monitoring and management through satellite as well as numerical based studies which is of immense relevance to coastal scientists and managers.

1. INTRODUCTION

Microwave remote sensing can be used to predict bathymetry at the depths between 10-70m. The day-night and all- weather capability of microwave satellite sensors such as SAR proves to advantageous, particularly in ocean applications (Singhroy, 1996). SAR is an active sensor that functions in the microwave regions of the electromagnetic spectrum and its basic principle involves transmitting and receiving microwave signals that are either reflected or backscattered from targets located on the surface of the earth. Microwave remote sensing based Synthetic Aperture Radar (SAR) datasets can be used for bathymetry retrieval by exploring the concept that when swell waves travel from deeper offshore regions to shallow near-shore waters, they are accompanied by changes in the wavelength and direction. Variable surface signatures are witnessed by virtue of changes in the underwater topography in the shallow water regions, that cause refraction, thereby aligning the waves parallel to the shoreline. The wave transformation phenomena (refraction and shoaling) are

traced from offshore to nearshore and depths are retrieved by applying suitable inversion techniques that involve the linear dispersion equation. A number of studies have been conducted to explore microwave remote sensing for depth estimation. Bell (1999) uses a series of radar images obtained from a marine radar working at a wavelength of 3cm. The author uses Holderness II data of three days to analyze the wave and subsequently compute depths, and the results clearly show that the tidal signals and the mean water levels obtained are comparable with those from an admiralty chart. Jin and Zhang (2000) use the L- band SIR-C images with HH polarization to derive bathymetry for an area of Hong Kong, China. They use an inversion algorithm based on continuity equation and the theory of weak hydrodynamic interactions to derive depths for this area. Fu and Fan (2007) estimate the coastal bathymetry by using the C band VV polarized SAR imagery of ERS-2 for a region in Wenzhou province in China by applying two main steps (1) spectrum analysis to derive wave number in both deep and shallow water, (2) utilizing the information of the wave parameters to derive water depth. Fan et al. (2008) suggest that in order to understand and extract depths from SAR imagery, it is imperative to derive a quantitative relationship between the relative normalized radar-backscattering cross-section (NRSC) and hydrodynamic modulation. This relationship is derived from the high frequency ocean spectrum balance equation and is used to develop a simulation model to analyze the optimum conditions required for shallow water depth estimation. A combination of Optical remote sensing data from Quick bird sensor and microwave remote sensing data from TerraSAR X of 1m resolution is used to derive bathymetry of an area near Rottnest island, Australia by Pleskachevsky et al. (2011). Similar to their study Brusch et al. (2011) estimate depths in the test sites of Philip near Melbourne (Australia) and Duck Research Pier in North Carolina by studying the ocean gravity waves on the SpotLight images of TerraSAR-X with a coverage of 10x10km. Most of these studies explore the use of waves for depth retrieval and the method is referred to as Wave Based Approach (WBA). Boccia et al. (2014) also use the wave based approach where the changes in the swell wave parameter is used to derive depths by applying the wave tracing method to calculate the swell wavelength and eventually the bathymetry. The method is applied on ALOS L- Band SAR data over Gulf of Naples, Italy. The resulting bathymetry shows a fair agreement with the values of water depth extracted from Nautical Charts provided by the Italian Navy Hydrographic Institute. Further, Boccia et al. (2015), analyses the main phenomenon governing the swell wave propagation responsible for bathymetry estimation. The linear dispersion equation is assessed and an error budge is developed to understand the various aspects of the wave based approach as well as its advantages and limitations. In a most recent study, Wiehle et al. (2019) develop a processor that automatically derives depth grid using the wave based approach. The authors report RMSD values of 6.5m in case of 10-20m depths; 6.7m in case of 20-30m depth and 7.7m for 30-40m depths.

An alternate approach to WBA is the current based approach (CBA) that works on the principle that the changes in the surface currents is due to the underlying topography which causes the intensity modulations witnessed in the SAR images (Renga et al., 2014). However, since modelling the variable parameters involved in CBA is computationally complex, WBA approach is generally considered more applicable than current based approach.

Therefore, the present research discusses the concept of SAR based bathymetry, illustrates the application of the Wave Based Approach for the coastal regions in India and reports the results obtained by comparing the obtained depths with those from GEBCO datasets and admiralty charts.

2. STUDY AREA

2.1 Coastal region along Maharashtra

The study region is situated along the Maharashtra coast between 73.07E and 73.14E &17.59N and 18.011N (Figure 1). Here, the dry season with little cloud cover, occurs in the months from December to March; April to May is a period of light winds whereas June to September is the duration of southwest monsoon when the winds are south-westerly and westerly. The tidal range decreases from the north to the south and so does the limit of the tidal incursion in the tidal rivers. In monsoon, waves exceeding 5m of height are seen especially towards the south Konkan. The wave heights decrease towards the north. In the fair weather however, wave heights do not exceed 2m.

The average peak period observed during monsoon is slightly greater than those recorded during non-monsoon periods with an average of 10.1 to 10.5 sec (Glejin et al., 2015).

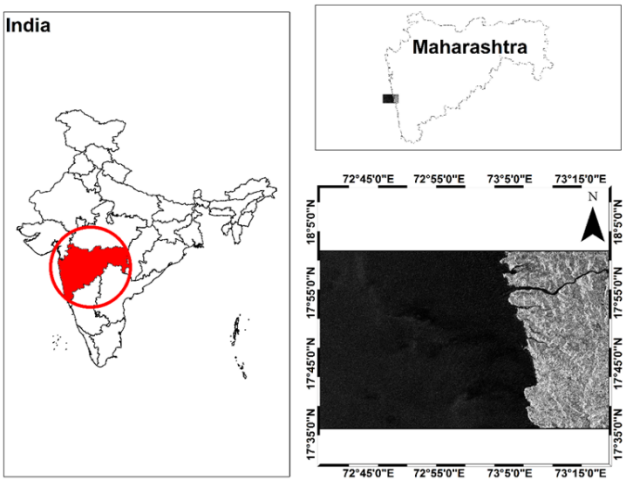

Figure 1 Study region along coast of Maharashtra

2.2 Coastal region along Puducherry

This study area is located between 79.87E and 79.79E longitude and 12.05N and 11.75N latitude, along the coast of Puducherry, East coast of India and is represented within a red rectangular box (Figure 2). The region is influenced by both south-west (SW) as well as north-east (NE) monsoon. The average significant wave height along the Puducherry coast is 0.9m and the average tidal range is between 0.7–0.8m. According to Kudale et al. (2004) because of the geographical situation of this coastal area this region experiences a greater frequency of cyclones, contrary to the west coast of India.

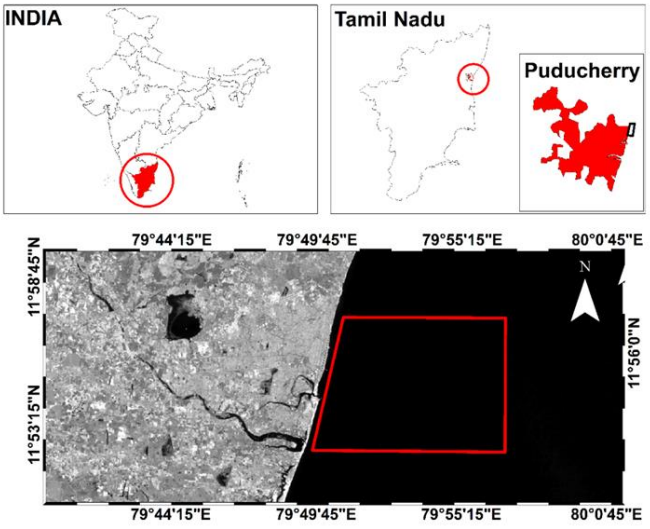

Figure 2 Study region along the coast of Puducherry

3. DATASET USED

3.1 Synthetic Aperture Radar

In this analysis, the bathymetry of the coastal region in Maharashtra and Puducherry are estimated using ALOS PALSAR Dual Pol HH polarized data of 12.5m resolution of 16th June 2007 and 26th January 2007 respectively. PALSAR is a Phased Array Type L-band Synthetic Aperture Radar that uses the L-band frequency in the microwave region and enables cloud free as well as day and night independent observations.

3.2 Calibration and Validation data

Hydrographic/ Admiralty charts

Admiralty chart datasets are used for the calibration and validation of the Wave based model for the study region located in Maharashtra. Various admiralty charts (No-492, 708, 1487, 1508, 1509, 2736, 3460, 3464, 4705 and 4706) are combined, and the depth values are digitized in ArcGIS environment to derive the resultant shapefiles (.shp). The shapefiles are primarily used for validating the SAR based depth retrievals.

GEBCO datasets

The GEBCO_2019 grid, released by the General Bathymetric Chart of the Oceans (GEBCO), is the latest and most widely used global bathymetric product on a 15 arc second grid.
The dataset provides value at the center of each grid cell, i.e. the depths are pixel center registered. (https://www.gebco.net/data_and_products/gridded_bathymetry_data/gebco_2019/gebco_2019_info.html).
The data is subset to derive depths for both the regions of interest.

4. METHODOLOGY

In general, it is suggested that if the conditions of linear imaging are satisfied, the Wave based approach (WBA) can be used to derive bathymetric information (Pleskachevsky et al. 2011). The examination of wave transformations is achieved by scanning the study area with a small window and by applying spectral analysis at each location within the window. Two main points have to be ensured for this analysis, firstly, the sea surface state should be fully characterized by the swell waves at the moment of SAR imaging, and secondly, the subset should be selected after proper visual inspection, so as to ensure that swell waves are present and visible in the SAR imagery. Resultantly, only those subsets of ALOS PALAR images of Mumbai and Puducherry are considered which clearly show strong intensity contrasts i.e. black and white stripping.
Figure 3 gives the general methodology followed for the bathymetry estimation using the linear dispersion equation.

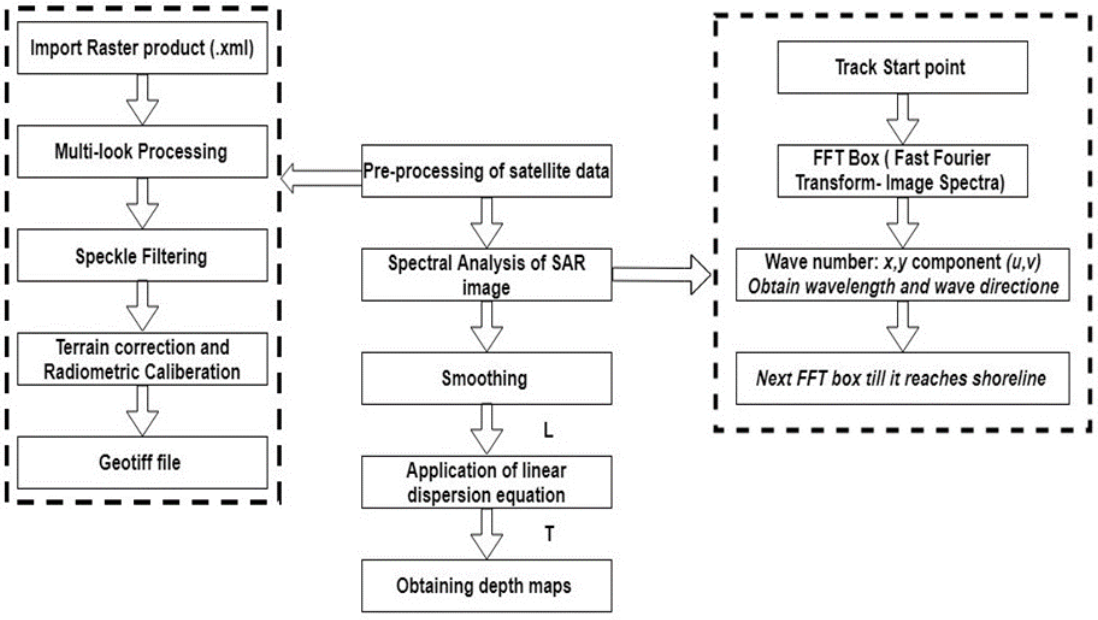

Figure 3 Flowchart of SAR based bathymetry estimation

4.1 . Preprocessing of SAR data

Taking into account the steps mentioned above the pre-processing steps carried out using the SNAP toolbox are explained below-

(1) Multi-look- The process involves generation of multiple look intensity images (power) by averaging over range and/or azimuth resolution cells. The intention is to improve the radiometric resolution of Single Look Complex (SLC) image. An intensity image made of squared pixels is the final product, obtained by considering the ground range resolution and azimuth pixel spacing.
(2) De-speckling- SAR images like those obtained from PALSAR sensor are affected by speckle (noise) which is defined are the statistical fluctuation associated with the radar reflectivity of each pixel in the scene. Speckle removal or de-speckling is conventionally performed by applying a filter, and for this analysis the 'Lee' filter is applied.
(3) Geo-coding and Radiometric Calibration- Generally, PALSAR captures an image by calculating the backscatter or ratio between the power of the pulse transmitted and the echo received. This ratio is projected into the slant range geometry, which is different when compared to images obtained through other modes or other radar sensors.
(4) In order to compare radar images geometric and radiometric calibration is a requirement. Here the calibrate and Terrain Correction tools are used.

4.2 Application of Wave Based Approach

The present method is a theory driven simplified algorithm that works on the assumption that SAR images swell waves perfectly without any disturbances. The WBA model involves two main processes (1) Spectral Analysis (2) Application of the linear dispersion equation. The aforementioned steps (1) and (2) are applied using a raster approach which includes moving a scanning window along the image axes. However, before the application of the moving window, certain pre-steps have to be considered. As the first step, it is a necessary to select the SAR images and sub-portions of the images in which swell waves are clearly visible. As mentioned earlier, this is confirmed by a visual check of the SAR images considered for the study. Following this, land must be masked out, as the approach cannot run over land pixels. The image is then resized by introducing a scaling factor, which is followed by the application of a 2D median filter. The filter considers the median value in the nearby neighborhood of any given pixel and uses it as the substitute amplitude value of the resized image pixels. Here, it is imperative to carefully select the optimum kernel size for the filter, in order to ensure the reduction of the noise and the preservation of the image modulations caused due to the presence of swell waves.
Hereafter, the raster scanning approach is utilized to perform spectral analysis which is basically the application of Fast Fourier Transformation technique (FFT) to obtain the peak wavelength and peak wave direction along each wave track. FFT is a useful method to decompose a function in spatial domain to the frequency domain and is very useful in deriving the regular periodicity in the image. The 2D image spectrum obtained by the application of FFT on a sub-image of N×N pixels consists of the peak in this spectrum, which represents the mean wavelength and the mean wave direction. The wave length and angle of propagation is estimated by using the following equations-

$$L_{WBA} = (N\Delta x)\sqrt{u^2 + v^2} \quad (1)$$

$$\theta = \arctan(\frac{v}{u}) \quad (2)$$

where, L_{WBA} is the measure peak wavelength, θ is the peak wave direction, Δx is the spatial resolution of the image, N is the size of the sub-image, u and v are coordinates of the dominant frequency with the center point as origin.

Further, the water depth *d* for a particular FFT box is retrieved from linear dispersion relation is given as follows-

$$d = \frac{L_{WBA}}{2\pi} \tanh^{-1}\left(\frac{2\pi L_{WBA}}{T^2 g}\right) \quad (3)$$

where, *T* is the wave period in (s), g is the gravitational constant.

As observed in this equation, the wave period is required for depth calculation. Generally, this can be measured by using a series of radar images, which may be practically difficult in the case of satellite remote sensing application. Alternatively, buoys or weather stations can be utilized. However, in the present case, the time period is obtained by applying the first guess approach. The swell period is computed offshore by using equation 3, wherein trial values of *T* are tested by comparing the derived value of water depths with the real values obtained from admiralty charts or GEBCO data. Although this approach has limited accuracy, it explores a significant property of dispersion relation which states that when the wave period is sufficiently long and local depths are small, the sensitivity of the depth to wave period is very low and hence greater uncertainties in wave period can be tolerated especially in the case of intermediate water (Boccia et al. 2015).

5. RESULTS AND DISCUSSIONS

For the case study regions of Maharashtra and Puducherry, the following steps are adopted;

- The original Maharashtra image with water pixels is of the dimension 5600*4700 pixels. The image is subset to the size 3495*3154 pixels. In case of Puducherry image, the dimensions of 2251*1747 pixels are reduced to 886*613. The data is basically resampled to 15m spatial resolution.
- A median filter with a kernel size 5×5 is applied on both the imageries.
- As explained earlier, the FFT method is used to retrieve the wavelength and wave direction and is applied on small boxes of the image subset along each track considered from offshore to the coastline. For both the case studies, a 128×128-pixels window box is utilized for FFT calculations. The FFT window is shifted by a uniform distance of 5 pixels (75m) starting from the first point until it approaches the coastline. The main problem faced during the FFT is applied within a small box, at a given point over the image, a single dominant peak is not obtained rather numerous peaks are observed. In order to choose the right peak, i.e. the peak corresponding to the track of the swell wave, limits have to be defined in the frequency domain. The algorithm ensures this by introducing a region of interest in the spectrum.
- The depth is then estimated by using the dispersion expression given in equation 3. The peak period *T* required to apply this equation is deduced by the assessment of the wave tracks.

5.1 Coastal Region along Maharashtra

The average wind speed during the acquisition of this data is between 7.04m/s (NOAA/NCDC Blended Daily Global 0.25° Sea Surface Winds, 1987-2011, Lon+/-180) and hence conducive to visually encounter swell wave in the imagery. Using the raster scanning method, it is observed that the swell wavelengths in the study region decreases as the wave moves from offshore towards the shoreline (Figure 4). The computed wavelengths are found to be in the range of 130–250m. The T_{MIN} obtained is 12.5s and the peak period calculated from the first guess approach is 13s. This value can also be substantiated with the help of available literature that suggests that the peak period during June to August is 13s (Nair and Kumar 2015).

The water depth encountered at the farthermost point offshore (approx. 47km away from shoreline) is estimated to be 45m.On further validation of these predictions with points (Figure 5) obtained from admiralty charts an R^2 value of 0.98 is obtained with an RMSE of 1.1m and MAE of 0.97m. Also on comparison with GEBCO data, the same points give an R^2 of 0.97 with an RMSE error of

1.34m and MAE of 1.1m. The final bathymetry map obtaining is shown in Figure 6.

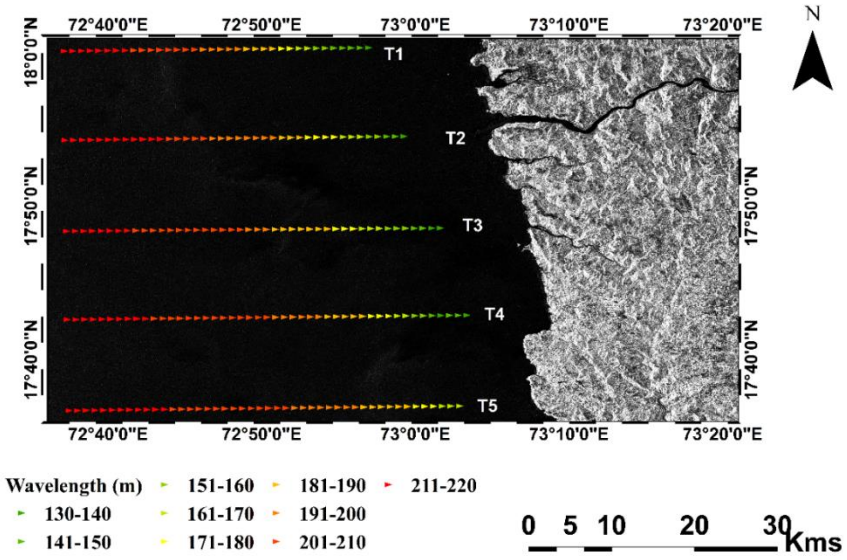

Figure 4 Showing change in wavelength offshore to near-shore for Maharashtra coast

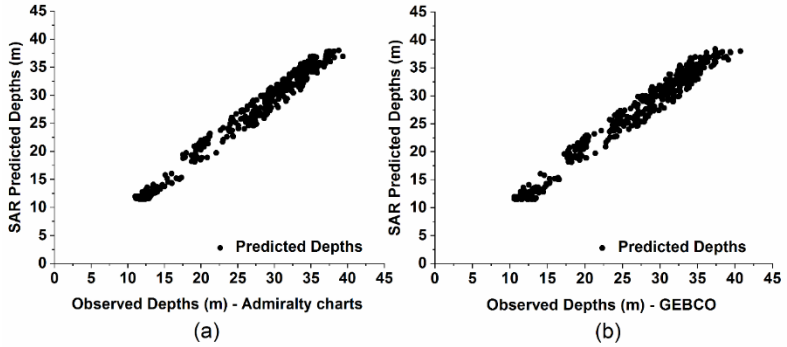

Figure 5 Plots showing comparison between (a) Observed depth from admiralty charts (b) Observed depths from GEBCO with SAR based predicted depths

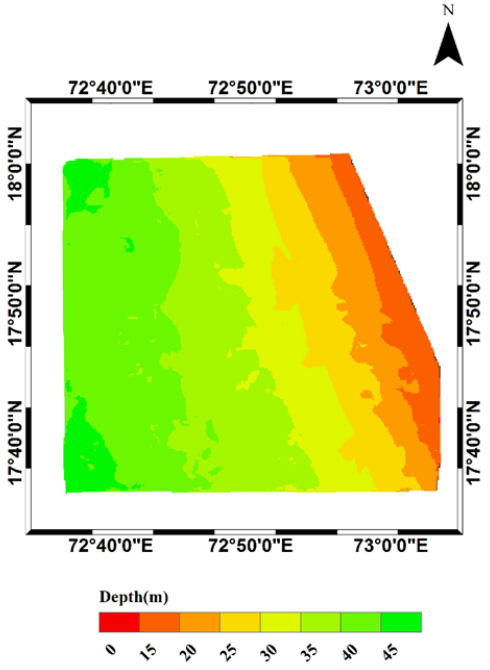

Figure 6 Bathymetry map obtained from wave based technique for Maharashtra region

5.2 Coastal Region along Puducherry

Limited wind speed data (NOAA/NCDC Blended Daily Global 0.25° Sea Surface Winds, 1987-2011, Lon+/-180) is available for this region depicting average speeds of 3.6m/s. According to Robinson (2004) Bragg scattering is possible at wind speeds above 3m/s and is sufficient to produce the intensity modulations that can be detected in SAR imagery as is also evident in the case of SAR imagery for the Puducherry region. The swell wavelength is calculated to be in the range of 120–250 m and decrease from offshore to shallow water region (Figure 7).

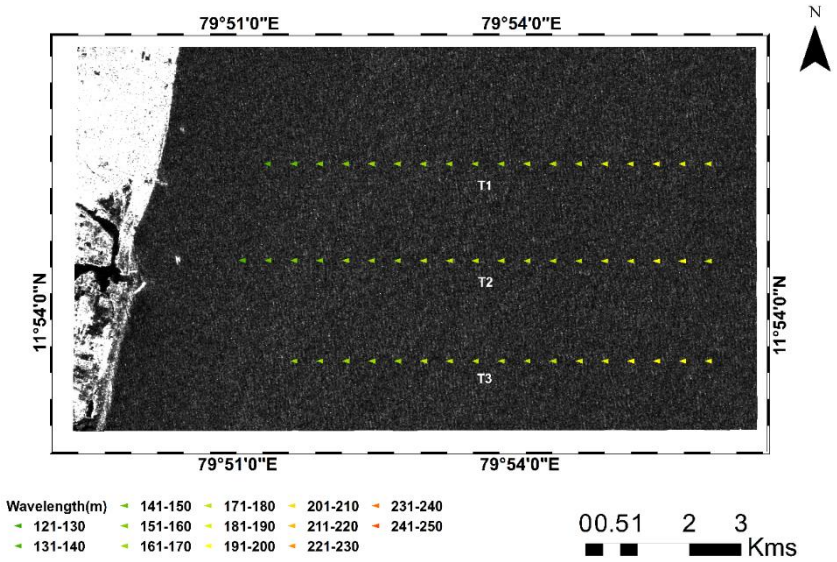

Figure 7 Showing change in wavelength offshore to nearshore for Puducherry coast

Similar to the estimations conducted for the Maharashtra case study, the peak period after track analysis and first guess is estimated to be 13s. This value of the peak wave period agrees with the findings of Sandhya et al. (2014) for the month of January 2007. The predicted water depth at the farthermost point, (almost 11 km away from the shoreline) is 30m. In order to validate the results, 195 points of predicted depths are compared with depths obtained from GEBCO (Figure 8). An R^2 value of 0.97 is obtained with an RMSE of 0.83m and MAE of 0.66m. Figure 9shows the final depth map for Puducherry.

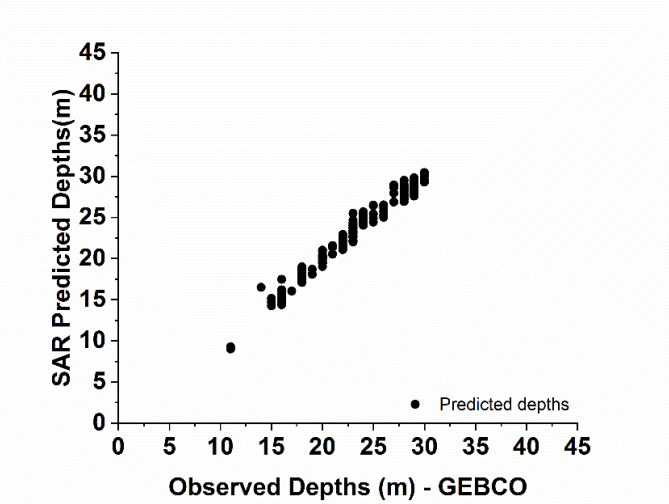

Figure 8 Plots showing comparison between observed depths from GEBCO with SAR based predicted depths

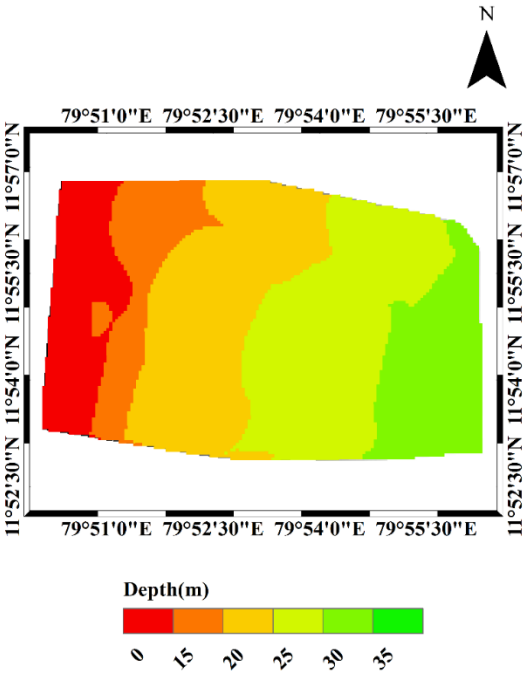

Figure 9 Bathymetry map obtained from wave based technique for Puducherry region

Based on the results obtained for both the case studies, it can be inferred that the wave tracing method can be used for SAR based retrieval of bathymetry. It is reported that SAR method can be exploited if swell waves are present in the wavelength range >80m (Brusch et al. 2010). Wavelength will be modified as long as the orbital velocity profile of the wave reach the sea bed and this takes place usually for depths less than 70m and wavelengths of 200m. The depth estimation from SAR basically happens in depth ranges of 10-70m and hence there is need to combine bathymetry retrievals from optical remote sensing which works in the depth range of 0-10m.

6. Conclusions

The present research involves application of Microwave remote sensing data for bathymetry estimation. SAR imagery has all weather capability and is not affected by clouds and hence can be used to estimate bathymetry especially during the period of rainfall. This can be an important tool to fill the bathymetry data gap during the monsoon seasons. However, the analysis is dependent on the availability of SAR data that clearly depicts waves in the imageries. The inconsistencies observed in the results are largely due to the lack or poor appearance of sea surface signature in the image. Nevertheless, it is evident from the study that SAR has the potential to provide depth information in the range of 10-70m.

7. References

Bell, P.S., 1999. Shallow water bathymetry derived from an analysis of X-band marine radar images of waves. Coastal Engineering, 37(3-4), pp.513-527.

Boccia, V., Renga, A., Rufino, G., Moccia, A., D'Errico, M., Aragno, C. and Zoffoli, S., 2014, July. L-band SAR image processing for the determination of coastal bathymetry based on swell analysis. In 2014 IEEE Geoscience and Remote Sensing Symposium (pp. 5144-5147). IEEE.

Boccia, V., Renga, A., Moccia, A. and Zoffoli, S., 2015. Tracking of coastal swell fields in SAR images for sea depth retrieval: Application to ALOS L-band data. IEEE Journal of selected topics in applied earth observations and remote sensing, 8(7), pp.3532-3540.

Brusch, S., Lehner, S., Schwarz, E., & Fritz, T., 2010. Near real time ship detection experiments. In SeaSAR 2010: Advances in SAR Oceanography from ENVISAT, ERS and ESA third party missions, Workshop ESA ESRIN, Frascati/Rome, Italy.

Brusch, S., Held, P., Lehner, S., Rosenthal, W. and Pleskachevsky, A., 2011. Underwater bottom topography in coastal areas from TerraSAR-X data. International Journal of Remote Sensing, 32(16), pp.4527-4543.

Fan, K.G., Huang, W.G., He, M.X., Fu, B. and Gan, X.L., 2008. Simulation study on the effect of wind on SAR imaging of shallow water bathymetry. Journal of Remote Sensing, 12(5), pp.743-749.

Fu, B. and Fan, K., 2007, November. Coastal water bathymetry derived from an analysis of SAR images of waves. In MIPPR 2007: Remote Sensing and GIS Data Processing and Applications; and Innovative Multispectral Technology and Applications (Vol. 6790, p. 679016). International Society for Optics and Photonics.

Glejin, J., Kumar, V.S. and Singh, J., 2015. Inter-annual variations in wave characteristics off Ratnagiri, Northeast Arabian Sea. Aquatic Procedia, 4, pp.25-31.

Jin, Y.Q. and Zhang, W., 2000, July. Inversion of underwater bottom topography by using the SAR imagery. In IGARSS 2000. IEEE 2000 International Geoscience and Remote Sensing Symposium. Taking the Pulse of the Planet: The Role of Remote Sensing in Managing the Environment. Proceedings (Cat. No. 00CH37120) (Vol. 5, pp. 1851-1853). IEEE.

Kudale, M.D., Kanetkar, C.N. and Poonawala, I.Z., 2004, December. Design wave prediction along the coast of India. In Proceedings of the Third Indian National Conference on Harbour and Ocean Engineering, NIO, Goa (Vol. 1, pp. 31-39).

Nair, M.A. and Kumar, V.S., 2016. Spectral wave climatology off Ratnagiri, northeast Arabian Sea. Natural Hazards, 82(3), pp.1565-1588.

Pleskachevsky, A., Dobrynin, M., Babanin, A.V., Günther, H. and Stanev, E., 2011. Turbulent mixing due to surface waves indicated by remote sensing of suspended particulate matter and its implementation into coupled modeling of waves, turbulence, and circulation. Journal of Physical Oceanography, 41(4), pp.708-724.

Renga, A., Rufino, G., D'Errico, M., Moccia, A., Boccia, V., Graziano, M.D., Aragno, C. and Zoffoli, S., 2014. SAR bathymetry in the Tyrrhenian Sea by COSMO-SkyMed data: A novel approach. IEEE Journal of Selected Topics in Applied Earth Observations and Remote Sensing, 7(7), pp.2834-2847.

Sandhya, K.G., Nair, T.B., Bhaskaran, P.K., Sabique, L., Arun, N. and Jeykumar, K., 2014. Wave forecasting system for operational use and its validation at coastal Puducherry, east coast of India. *Ocean Engineering*, *80*, pp.64-72.

Singhroy, V., 1996. Interpretation of SAR images for coastal zone mapping in Guyana. Canadian Journal of Remote Sensing, 22(3), pp.317-328.

Wiehle, S., Pleskachevsky, A. and Gebhardt, C., 2019. Automatic bathymetry retrieval from SAR images. CEAS Space Journal, 11(1), pp.105-114.